

Schematic relief of the near-surface and deep-seated magnetic basement, using local-power spectra, Gabal El-Erediya area, Eastern Desert, Egypt

AHMED A. AMMAR and SAID I. RABIE

Nuclear Materials Authority, P.O. Box 530, Cairo, Egypt

(First received 11 May, 1990; revised form received 21 May, 1991)

Abstract - The use of Fourier's transformation and the representation of magnetic anomalies in the form of frequencies (power-spectra) have enabled a thorough analysis of the magnetic anomalies and the estimation of depths at which their source exist. The method applied computes the spectrum of anomalies in the potential (magnetic) field from the data of a profile and of a two-dimensional map. The average interpreted depths from the power spectrum are assigned to the centre of the profile and to the center of the map.

As an example, the interpretation of the total aeromagnetic survey of Gabal (G.) El Erediya area, Eastern Desert, Egypt was tried. The two average depths estimated for the near-surface and deep-seated interfaces using the profiles in both the N-S and E-W directions are 0.55 and 1.60 km, while those estimated using the two-dimensional map are 0.59 and 1.31 km respectively. It was found that the area under study consists of a series of simple and complex alternating NW-SE and ENE-WSW trending horsts (or uplifted blocks) and grabens (or downfaulted blocks). The previous trend parallels the Red Sea and some segments of the River Nile, while the latter trend parallels the shear zone of Safaga-Qena. The shorter wavelength (ENE) seems to suffer rejuvenation, i.e., more than one tectonic event and is consequently more ancient. Meanwhile, the longer wavelength (NW) appears to undergo only one tectonic event and is accordingly more recent.

INTRODUCTION

Fourier analysis is often used for the estimation of the depth of magnetic bodies in the earth's crust (Battacharyya and Raychaudhuri, 1967; Naidu, 1970; Spector and Grant, 1970; Spector, 1971; Syberg, 1972). This is accomplished by digitizing and Fourier-transforming the values of the field anomalies of one component, usually the field-parallel component ΔT , over a finite area, preferably a square. From this transform, some sort of a spectrum is drawn (amplitude or power spectrum) and plotted on a logarithmic scale for the amplitude versus a linear scale for the frequency. The spectra in these graphs often show frequency intervals where the logarithms of the amplitudes may well be represented by a linear function of the frequency, where the amplitudes decrease with increasing frequency.

As an example, the depths from aeromagnetic anomalies were estimated of El Erediya area, Central Eastern Desert, Egypt (Fig. 1).

GEOLOGICAL BACKGROUND

Gabal (G.) El-Erediya area, Central Eastern Desert, Egypt consists of rocks ranging in age from Precambrian I to Quaternary. It is covered by igneous and metamorphic basement complex in its eastern portion, and Phanerozoic Sediments (Fig. 2).

The area under study is characterized by the existence of huge granite plutons acquiring one principal direction, NW-SE (Ammar, 1973). This trend includes G. El Erediya, G. Maghrabiya, G. El Gidami, G. Ria El Gerra and G. El Misikat. Other detached masses as G. Kab Amri and G. Um Had were also observed. Metavolcanics of basic to ultrabasic composition occur between and around these granite masses and plutons. Metasediments exist in a rather limited areal extension at the eastern and southern parts of the area under consideration. The western parts of this area is occupied by Nubian Sandstone formation, which represents the base of the Phanerozoic cover sediments (El Kasas, 1974; Bakhit, 1978 and Mostafa, 1979).

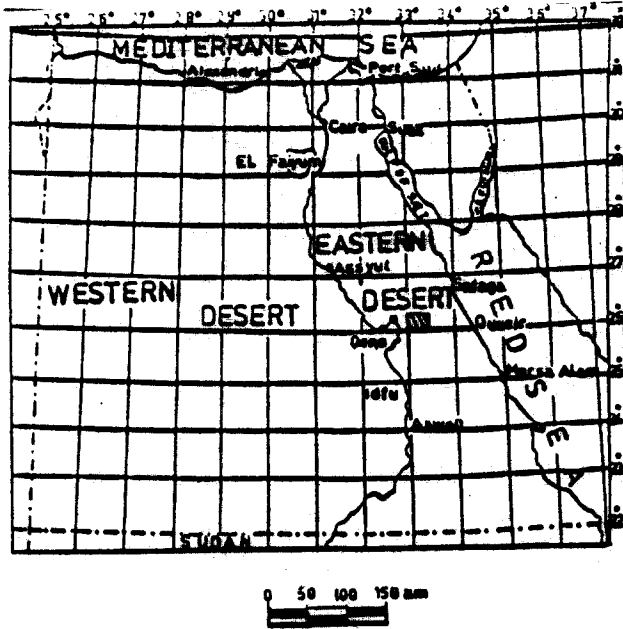


Fig. 1. Location map of the area under study.

METHOD

The total aeromagnetic field (Fig. 3) in the interpreted area was digitized on a square grid of a density which guarantees that all details necessary for the given interpretation task are included (1.0 x 1.0 km).

Based on the results obtained in their studies, Spector and Battacharayya (1966); Spector and Grant (1970); Cianciara and Marcak (1975), an averaged power spectrum from a certain area can be recorded in the following mode:

$$S(w) = \sum_{k=1}^p \alpha_k \cdot S_k(w) \dots\dots\dots(1)$$

Where $S(w)$ is the power spectrum anticipated value, w is the frequency, and p is the number of interfaces.

The functions $S_k(w)$ that appear in the formula (1) are related to the average depth of occurrence of the disturbing surface as in the following inter-relations:

$$S_k(w) \approx e^{-h_k(w)} \dots\dots\dots(2)$$

where h_k is the depth down to the k -th horizon of the disturbance. Instead, the coefficients α_k are interpreted as the weights (contributions) of the k -th disturbing horizon to the field.

As arises from practical calculations, the weights (contributions) of α_k as present in the decomposition (1) are increasing exponentially along with an

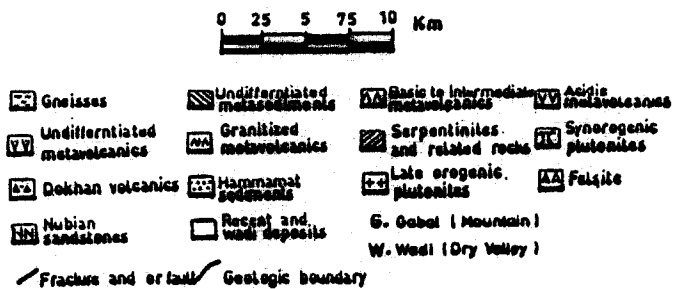
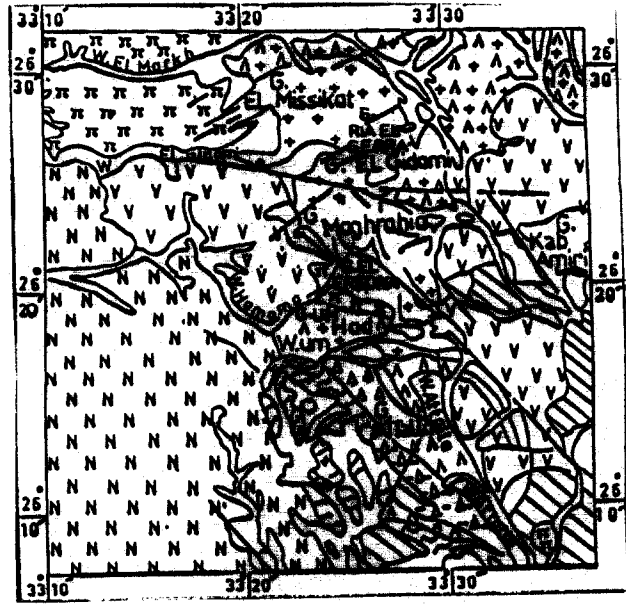


Fig. 2. Compiled geological map of El-Eredtya area Central Eastern Desert, Egypt. (after Ammar, 1974; Bakhit, 1978; Mustafa, 1979)

increase in k (number of disturbing horizon, counting from the top), whereas for an established horizon they are of the same order.

That inference eases significantly the interpretation of the local power spectrum. It allows to ascribe the interpreted depths to the respective horizon of the disturbance. The method concerned has been used to determine the depth of a surface on which there is a principal rapid transition of the physical variables: density and magnetic susceptibility.

It can be seen that there are spectra showing more than one interval where $S(w)$ has a quasi-linear dependence on (w) , but with a different slope in each interval.

A spectrum with two such intervals must be expected, e.g., over an arrangement of magnetic sources which occur at two different interfaces (depths), where the sources at the greater depth are stronger. On the measuring plane, each of these layers of magnetic sources would alone produce a linear spectrum. The spectrum of the upper interface dips more gently, the spectrum of the lower interface more steeply (Hahn *et al.*, 1976).

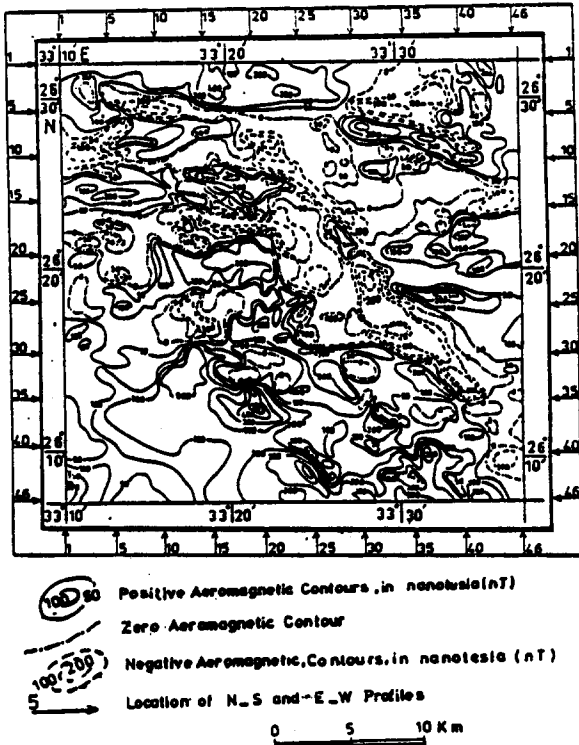


Fig. 3 Total aeromagnetic map of El-Erediya area, Central Eastern Desert, Egypt.

Figure 3 presents the map of the total-intensity aeromagnetic anomalies of Gabal (G.) El-Erediya area (46 x 46 km), Eastern Desert, Egypt.

The surveyed area was flown over at an average altitude of 70 m with profiles directed N60°E and spacing of 500 m. The data which are analysed here were digitized in an E-W direction, along a square grid, with an elementary spacing of 1.0 km.

The amplitude of the power spectrum of the whole matrix (46 x 46 km) of the surveyed area was calculated, drawn (Fig. 4) and two depth interfaces were computed.

Besides, the power spectrum and the depths for the 20 interpreted profiles (10 N-S and 10 E-W profiles with 5 km spacing) of the aeromagnetic data of the area under study were computed automatically (Fig. 5). The results of the N-S profiles illustrate the variation in depth in the E-W direction at the midpoint of every profile and vice versa.

RESULTS AND DISCUSSION

The results of estimation of the depths of the near-surface and deep-seated interfaces, obtained from the application of the technique of power spectrum to the 20 interpreted total aeromagnetic profiles (10 E-W and 10 N-S) of the Gabal (G.) El-Erediya area, Eastern Desert, Egypt are shown in Table I.

The aeromagnetic map of the area under investigation (Fig. 3) can be divided into two parts of differing magnetic character, a magnetically-

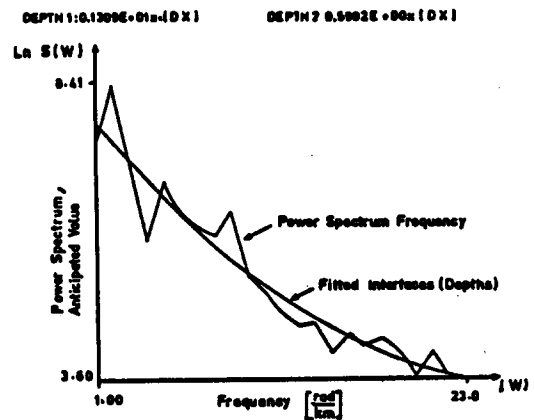


Fig. 4. Local power spectrum from interface determination of G. El-Erediya area, Central Eastern Desert, Egypt.

calm portion with smooth contours and low magnetic relief best developed in its western side and a magnetically-complex portion with steep gradients and high magnetic relief best developed in its eastern side, where the latter portion occupies the biggest part of the study area. Correlation of the magnetic intensities with exposed rocks shows that the magnetically-quiet portion coincides with the Nubian Sandstones and shales, while the magnetically-complex portion conforms with the Precambrian basement complex.

The total aeromagnetic data show a system of distinct, linear and relatively large amplitude magnetic anomalies in the area under study.

Table I. The results of estimation of the depth of the near- and deep-seated interfaces, G.El-Erediya area, Eastern Desert, Egypt.

Ser. No.	Prof. No.	Dir.	Depth. km		Near-surface interface		Deep-seated interface	
			E-W	N-S	E-W	N-S	E-W	N-S
1	1		0.3	0.7	2.8	0.7		
2	5		0.0	0.2	1.3	1.3		
3	10		0.1	0.5	0.7	2.1		
4	15		0.5	0.4	0.5	0.9		
5	20		0.0	1.4	1.6	2.3		
6	25		0.4	1.4	3.6	1.4		
7	30		0.4	1.9	2.4	2.3		
8	35		0.4	0.5	1.3	1.6		
9	40		0.4	0.4	0.5	1.2		
10	46		0.7	1.0	2.6	1.3		
Average depth in km	Profile data		0.3	0.8	1.7	1.5		
	2-dimensional data		0.55		1.60			
	2-dimensional data		0.59		1.31			

Ser. No. = Serial number
Prof. No. = Profile number.

Prof. Dir. = Profile direction

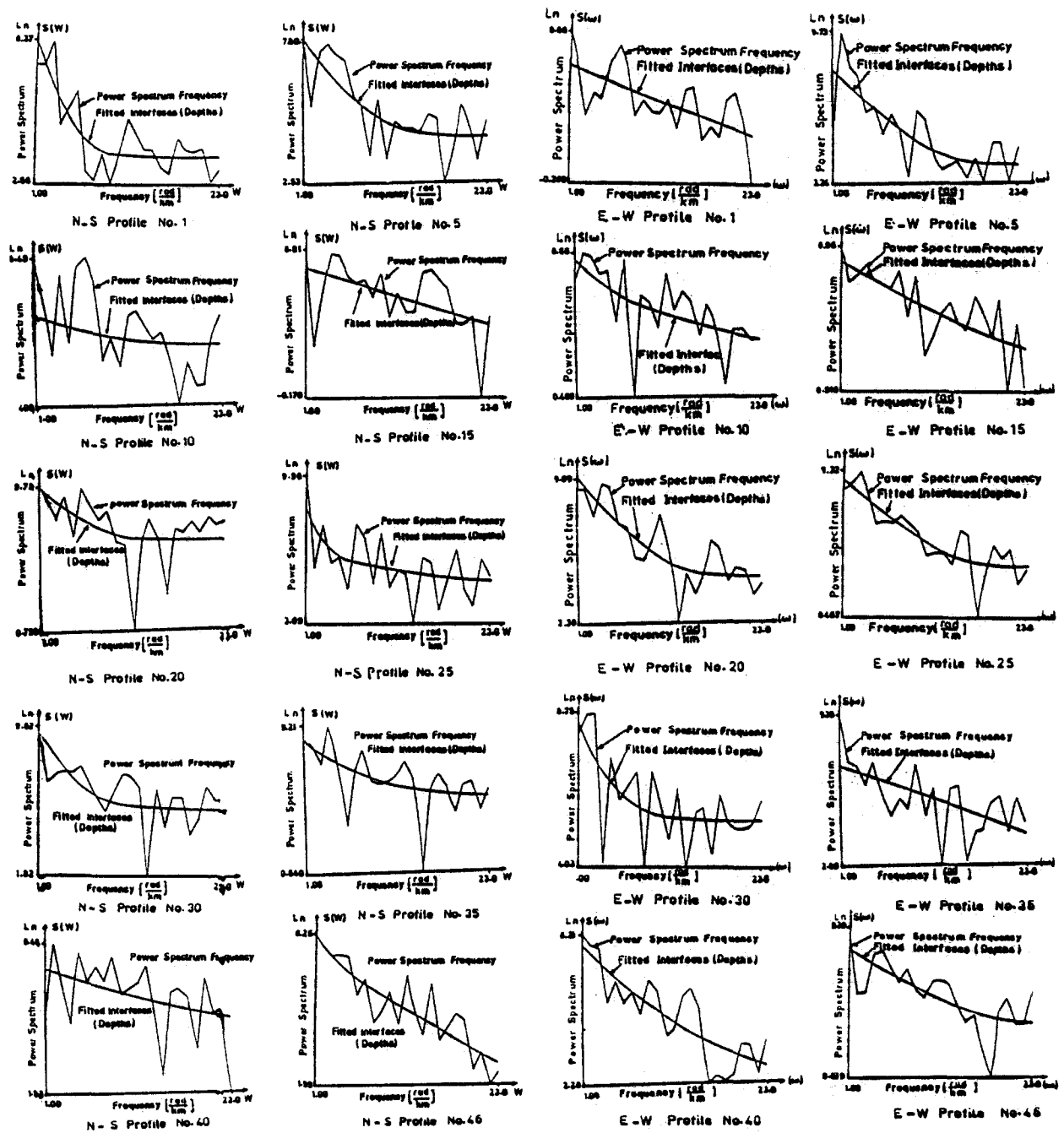


Fig. 5. Local power spectra and fitted interfaces (depths) of the 10 N-S and the 10 E-W profiles, G. El-Erediya area, Eastern Desert, Egypt.

These linear anomalies strike in a NW-SE direction parallel to the Red Sea as well as to some segments of the River Nile. Krs *et al.*, 1973, stated that such these linear magnetic anomalies are characteristic by the presence of deep-seated tectonic zones (features) on the earth. These linear anomalies were verified by ground geophysical methods (Krs *et al.*, 1973), and were found to be caused by dykes containing many ferromagnetic components. Study of the ERTS-1 Satellite images by El Shazly *et al.* (1973b) extended these linear features as far as the Nile Valley.

The total aeromagnetic data also show an elongated major negative magnetic zone located in the mid portion of the area under study and trending in a NW direction. It was found to coincide mainly with the rocks of Late Orogenic Plutonites (red and pink granites).

The schematic relief (Fig. 6A and B) of the area under consideration shows that the estimated depth of the near-surface interface ranges from zero till 1.9 km, while that of the deep-seated interface oscillates between 0.5 and 3.6 km.

The two average estimated depths of the near-surface interface in both the E-W and N-S directions are nearly 0.3 and 0.8 km respectively. Meanwhile, the two average estimated depths of the deep-seated interface in both the E-W and N-S directions are 1.7 and 1.5 km respectively. The average estimated depth for the near-surface interface of the whole area is 0.55 km, while that of the deep-seated interface of the whole area is 1.60 km. The latter two results estimated using the 20 profiles separately conform largely with the two results (0.59 and 1.31 km) obtained applying the power spectrum to the 2-dimensional magnetic data collectively (Fig. 4). This means that the method is successful in estimating the depths when using either the profiles or the 2-dimensional data, a result which is evident when comparing the previous 4 results.

The schematic relief of the deep-seated interface along the central E-W profile (Fig. 6B) shows distinct and simple alternating series of NW-trending horsts and grabens (or uplifted and downfaulted blocks) with approximately 31 km wavelength. They are almost parallel to the Red Sea graben and many segments of the course of the River Nile Valley (graben?).

Besides, the schematic relief of the deep-seated interface as seen from the central N-S profile (Fig. 6A) shows less distinct and less simple alternating ENE trending horsts and grabens (or uplifted and downfaulted blocks), almost parallel to the

shear zone extending from Safaga on the Red Sea Coast to the great bend of the River Nile at Qena with nearly 14 km wavelength, which is about one half the previously-stated wavelength.

Because of the relationship of the wavelength of horsts occurrence (or uplifted blocks) and grabens (or downfaulted blocks), it could be assumed that the shorter wavelength (ENE-trend) has suffered more than one tectonic event in approximately the same direction, (i.e., reactivation or rejuvenation), and is supposed to be more ancient. Meanwhile, the longer wavelength (NW-trend) has undergone only one tectonic event, whose effect is still clear, and is believed to be more recent, and consequently, affected the previous (shorter) wavelength (ENE-trend). Nevertheless, these relative wavelengths of the basement topography are not sufficient evidence to deduce the relative timing of events, yet they are consistent with other evidences from the structural history of Egypt as interpreted by many authors of this field from NE Africa and Arabia.

The schematic relief of the near-surface interface along the central E-W profile (Fig. 6B) shows approximately gentle relief except at the contact between the basement complex and the sedimentary cover, where the depth reaches 0.5 km. This is the same depth as the schematic relief of the deep-seated interface along the central E-W profile, and conforms well with a NW-trending wadi (dry valley). From this point, eastwards and westwards, the depth approximates zero km, then it goes deeper in both directions especially eastwards. There is another point at the same profile, eastwards, where the depth is nearly the same for both interfaces. It also coincides with a NW-trending wadi (dry valley). Both points conform well with the crest of two interpreted horsts or uplifted blocks. Generally, the schematic relief of the near-surface interface does not conform well with the relief of the deep-seated interface along the control E-W profile.

The schematic relief of the near-surface interface along the central N-S profile (Fig. 6A) shows a fairly good similarity with that of the deep-seated interface. This may be a sign that the near-surface has also been subjected to reactivation (or rejuvenation) with the deep-seated ENE-trending tectonics. There are 2 points where the depth of the near-surface and the deep-seated interface equalize. The northern point coincides with a major E-W fault as well as a wadi (dry valley), while the approximately central one is located within the metavolcanics and could be located at the extension of a NE-trending fault. It is worthy to mention that the ENE-tectonics is strongly represented in this area due to the presence of a major shear zone (Qena-Safaga shear zone) at its northern part.

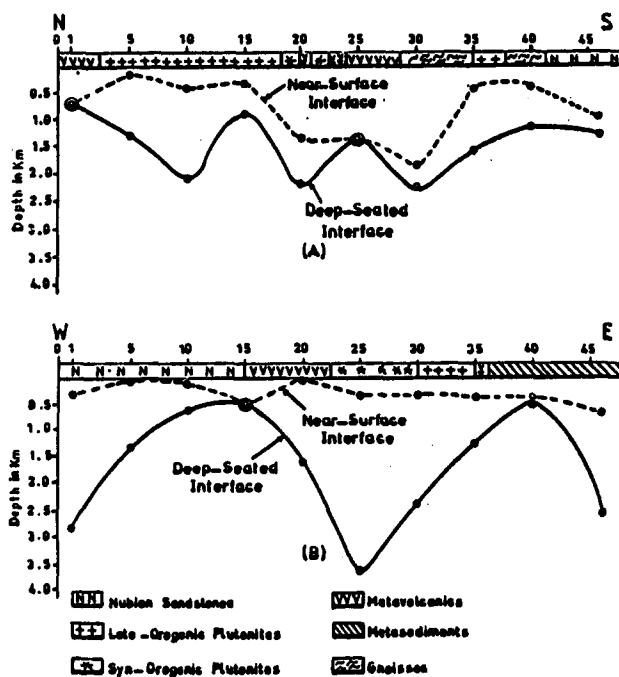


Fig. 6. Schematic relief of the near-surface (-----) and the deep-seated (—) interfaces along the N-S central profile as computed from the E-W profiles (A) and along the E-W central profile as computed from the N-S profiles (B) correlated with the geologic central cross sections, G. El-Erediya area, Eastern Desert, Egypt.

CONCLUSIONS

El-Erediya area, Eastern Desert, Egypt consists of relatively simple and obvious alternating series of NW-trending horsts and grabens (uplifted and downfaulted blocks) with approximately 31 km wavelength, that are parallel to the Red Sea graben and some segments of the course of the Nile Valley (graben?).

Besides, the area under study is composed of relatively complex and vague alternating ENE trending horsts and grabens (uplifted and downfaulted blocks), with nearly 14 km wavelength, which reaches about half the previously-stated wavelength. They are parallel to the two well-known shear zones of the Eastern Desert of Egypt extending from Safaga and Mersa Alam on the Red Sea Coast to the great bend of the River Nile at Gena and Aswan respectively. Both series are approximately perpendicular to each other.

It could be assumed that the shorter wavelength of the occurrence of (ENE) series has suffered more than one tectonic event in the same direction. Meanwhile, the longer wavelength of the occurrence of (NW) series has undergone only one tectonic event, whose consequence is still clear, and affected the previous ENE series. Consequently, the NW series seems to be younger than the ENE series, a result which agrees well with that has been reached by many workers in this field.

The two average computed depths or the near-surface and deep-seated interfaces for the area under consideration were 0.55 and 1.60 km using the profiles, and 0.59 and 1.31 km using the two-dimensional data respectively.

REFERENCES

- Ammar, A. A. 1973. Application of Aerial Radiometry to the Study of the Geology of Wadi El Gidami Area, Eastern Desert, Egypt (With Aeromagnetic Application). Ph.D. Thesis, Univ. of Cairo, Giza, Egypt. 424 p. (unpublished.)
- Bakhit, F. S. 1978. Geology and radioactive mineralization at G. El-Missikat Area, Central Eastern Desert, Egypt. Ph.D. Thesis, Univ. of Ain Shams, Cairo, Egypt, 289 p. (unpublished).
- Bhattacharya, B. K. and Raychaudhuri, B. 1967. Aeromagnetic and geological Interpretation of a section of the Appalachian Belt in Canada. *Can. J. Earth Sci.* **4**, 1015-1037.
- Cianciara, B. and Marcak, H. 1975. Interpretation of Gravity Anomaly by the Means of Local Power Spectra. *Geophysical Prospecting* **24**, 273-286.
- El Kassas, I. A. 1974. Radioactivity and Geology of Wadi Atalla Area, Eastern Desert, Egypt. Ph.D. Thesis, Univ. of Ain Shams, Cairo, Egypt, 502 p. (unpublished).
- El Shazly, E. M., Abdel Hady, M. A., El Ghawaby, M. A. and El Kassas, I. A. 1973b Geologic Interpretation of ERTS-1 Satellite Images for East Aswan Area, Egypt. Proceedings of the Ninth International Symposium on Remote Sensing of Environment, Research Institute of Michigan, An Arbor, Michigan, 105-117.
- Hahan, A., Kind, E. G. and Mishra, D. C. 1976. Depth estimation of magnetic sources by means of Fourier amplitude spectra. *Geophysical Prospecting* **24**, 287-308.
- Krs, M., Soliman, A. A. and Amin, A. H. 1973 Geophysical phenomena over deep-seated tectonic zones in southern part of Eastern Desert of Egypt. *Annals Geol. Surv. Egypt* **II**, 125-138.
- Naidu, P. S. 1970. Fourier Transform of large scale aeromagnetic fields using a modified version of Fast Fourier Transform. *Pageoph.* **18**, 17-25
- Spector, A. 1971. Aeromagnetic map interpretation with the aid of the digital computer. *CIM Bull.* **64**, 27-33.
- Spector, A. and Bhattacharya, B. K. 1966. Energy density spectrum and autocorrelation function of anomalies due to simple magnetic models. *Geoph. Prosp., Holland*, **XIV**, 3
- Spector, A. and Grant, F. S. 1970. Statistical models for interpreting aeromagnetic data. *Geophysics* **35**, 293-302.
- Syberg, F. J. R. 1972. A Fourier method for the regional residual problem of potential fields, *Geophys. Prosp.* **20**, 47-75.